





Locking of magnetization and Josephson oscillations at ferromagnetic resonance in a φ_0 junction under external radiation

S. A. Abdelmoneim ^{1,2}, Yu. M. Shukrinov ^{1,3,4}, K. V. Kulikov ^{1,3}, H. ElSamman,² and M. Nashaat ^{1,5,*}

¹*BLTP, JINR, Dubna, Moscow Region 141980, Russia*

²*Physics Department, Menoufia University, Faculty of Science, 32511 Shibīn al Kawm, Egypt*

³*Department of Nanotechnology and New Materials, Dubna State University, Dubna 141980, Russia*

⁴*Moscow Institute of Physics and Technology, Dolgoprudny, 141700 Moscow Region, Russia*

⁵*Department of Physics, Faculty of Science, Cairo University, 12613 Giza, Egypt*



(Received 17 January 2022; revised 13 April 2022; accepted 21 June 2022; published 6 July 2022)

We demonstrate the locking of magnetic precession in the φ_0 Josephson junction by external electromagnetic radiation through the locking of the Josephson oscillations in the ferromagnetic resonance region. This leads to a step in the dependence of the magnetization on the bias current. The step's position is determined by the radiation frequency and the shape of the resonance curve. In junctions with a strong spin-orbit coupling, states with negative differential resistance appear on the IV characteristic, resulting in an additional locking step. We show that the corresponding oscillations have the same frequency as the oscillations at the first step, but they have a different amplitude and a different dependence on the radiation frequency. This makes it possible to control not only the frequency but also the amplitude of the magnetic precession in the locking region. It opens up unique perspectives for the control and manipulation of magnetic moment in hybrid superconducting systems.

DOI: [10.1103/PhysRevB.106.014505](https://doi.org/10.1103/PhysRevB.106.014505)

I. INTRODUCTION

The φ_0 junction related to a special class of anomalous Josephson structures with coupled superconducting and magnetic characteristics allows the manipulation of magnetic properties by Josephson current [1–6]. It demonstrates a number of interesting features important for superconducting spintronics and modern informational technologies [7–22]. The current-phase relation of the φ_0 junction is given by $I = I_c \sin(\varphi - \varphi_0)$, where the phase-shift φ_0 is proportional to the magnetic moment perpendicular to the gradient of the asymmetric spin-orbit potential [23,24]. Superconductor spintronics, based on anomalous Josephson junctions, have evolved into a major field of research that broadly encompasses different classes of materials, magnetic systems, and devices [5,25–40]. Recently, an anomalous phase shift was experimentally observed in different systems, particularly in the φ_0 junction based on a nanowire quantum dot [41] and directly through CPR measurement in a hybrid SNS JJ fabricated using Bi_2Se_3 [which is a topological insulator with strong spin-orbit coupling (SOC)] in the presence of an in-plane magnetic field [42]. The observation of a tunable anomalous Josephson effect in InAs/Al Josephson junctions measured via a superconducting quantum interference device (SQUID) was reported in Ref. [43]. The authors were able to tune the SOC of the Josephson junction by more than one order of magnitude. This gives the ability to tune φ_0 and opens several new opportunities for superconducting spintronics [5] and new possibilities for realizing and characterizing topolog-

ical superconductivity [44–46]. In Refs. [47,48], the authors argued that the φ_0 Josephson junction is ideally suited for studying quantum tunneling of the magnetic moment.

Though the static properties of the SFS structures are well studied both theoretically and experimentally, much less is known about the magnetic dynamics of these systems [36,49–60]. Different types of very simple and harmonic precessions of the magnetic moment were demonstrated in Ref. [61]. It is expected that external electromagnetic radiation would lead to a series of novel phenomena. The possibility of the appearance of half-integer Shapiro steps (SS), in addition to the conventional integer steps, and the generation of an additional magnetic precession with frequency of external radiation was already discussed in Ref. [24].

Nonlinear superconducting structures exhibit a negative differential resistance (NDR) in the current-voltage characteristics [62,63], which plays an essential role in many applications, in particular for THz radiation emission [64–73]. Here we demonstrate an important role of the states with NDR in the locking of magnetization and Josephson oscillations at ferromagnetic resonance (FMR).

In this paper the IV characteristics (IVC) and magnetization dynamics of the φ_0 Josephson junction under an external electromagnetic radiation are studied. We solve a system of Landau-Lifshitz-Gilbert-Josephson equations that take into account the interaction of Josephson oscillations and the magnetic moment of the ferromagnetic layer. The bias current dependence of maximal magnetization component $m_y^{\max}(I)$ (taken at each value of bias current) manifests two phenomena, such as FMR and locking of the magnetization precession to the oscillations of the external field through the locking to the Josephson oscillations. The locking is manifested as a step

*majed@sci.cu.edu.eg

on $m_y^{\max}(I)$ dependence and its maximum shows the FMR. We clarify the role of SOC in the appearance of the nonlinearity in the IV curve and additional SS at small radiation amplitudes. We show that in junctions with a strong SOC the states with NDR result in an additional step with corresponding oscillations having the same frequency as the oscillations at the first step, but a different amplitude and different dependence on the radiation frequency. This opens a unique way to control not only the frequency but also the amplitude of the magnetic precession in hybrid superconducting systems.

The rest of the paper is as follows. In Sec. II, we describe the model and present its parameters. The results of our simulations are presented in Sec. III. In Sec. III A we discuss nonlinear features in the IVC due to SOC. Next, in Sec. III B we demonstrate the locking of the magnetic moment precession by external radiation. The characteristic features of the locking phenomenon are described in Sec. III C and Sec. III D. Finally, we conclude in Sec. V.

II. MODEL AND METHOD

In φ_0 junction the spin orbit plays the role of coupling between the Josephson current and magnetization. One example of SOC is the Rashba SOC [74–76] with a Hamiltonian given by $\alpha_{so}\boldsymbol{\sigma} \cdot [\mathbf{p} \times \nabla U(\mathbf{r})]$, where α_{so} is the Rashba parameter, $\boldsymbol{\sigma}$ are the Pauli matrices, $U(r)$ is the lattice potential experienced by the electrons, and \mathbf{p} is the momentum operator. Using the Ginzburg-Landau (GL) approach, the author in Ref. [23] shows that the current phase relation in φ_0 junction reads as

$$I = I_c(\varphi_0) \sin(\varphi - \varphi_0) = 4e\gamma |\Delta|^2 e^{-2L\sqrt{\frac{a}{\gamma} - \tilde{\epsilon}^2}} \sqrt{\frac{a}{\gamma} - \tilde{\epsilon}^2} \sin(\varphi - \tilde{\epsilon}L), \quad (1)$$

where φ is the phase difference between the superconducting electrodes; φ_0 is characterized by the SOC parameter and internal exchange field [23,24]; γ, a are the coefficients of GL equation; Δ is the gap energy; $\tilde{\epsilon} = \alpha_{so}h/\gamma$, α_{so} is the SOC strength; and h is the internal exchange field (we have the negative sign inside the sine function in contrast with Ref. [23] due to the direction of the y axis, which is reversed in our case). The condition $a/\gamma > \tilde{\epsilon}^2$ assures that the weak link is in the normal state [23]. Generally, the critical current depends on the SOC and the internal exchange field in the ferromagnetic layer. In this paper, we concentrated on the locking phenomena and assume $a/\gamma \gg \tilde{\epsilon}^2$; thus the critical current does not change significantly with SOC or exchange field.

The geometry of the considered φ_0 is shown in Fig. 1(a). The ferromagnet easy axis and the gradient of the spin-orbit potential (n) are directed along the z axis. In this case $\varphi_0 = rh_y$, where $r = L\alpha_{so}/\gamma$. In Josephson junctions with a thin ferromagnetic layer the superconducting phase difference and magnetization of the F layer are two coupled dynamical variables. The system of equations describing the dynamics of these variables is obtained from the Landau-Lifshitz-Gilbert (LLG) equation and Josephson relations for current and phase difference.

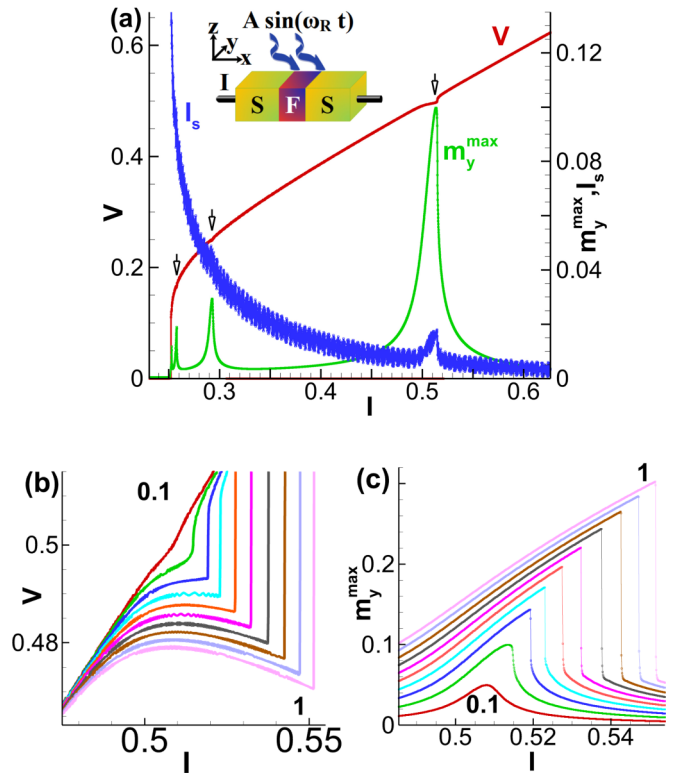


FIG. 1. (a) Manifestation of the FMR in $m_y^{\max}(I)$, IVC, and $I_s(I)$ for the φ_0 junction which geometry is shown in the inset with S, superconductor; F, ferromagnet. Simulation parameters were $G = 0.01$, $r = 0.2$, and $\alpha = 0.01$. (b) Enlarged parts of IV curves in the resonance region at different r . The numbers indicate the increasing of SOC from 0.1 to 1 by an increment 0.1. (c) The same for $m_y^{\max}(I)$.

The total system of LLG-Josephson equations [24] (to be used in our numerical studies) in normalized units is given by:

$$\begin{aligned} \dot{m}_x &= \frac{\omega_F}{1 + \alpha^2} \left\{ -m_y m_z + Grm_z \sin(\varphi - rm_y) \right. \\ &\quad \left. - \alpha [m_x m_z^2 + Grm_x m_y \sin(\varphi - rm_y)] \right\}, \\ \dot{m}_y &= \frac{\omega_F}{1 + \alpha^2} \left\{ m_x m_z \right. \\ &\quad \left. - \alpha [m_y m_z^2 - Gr(m_z^2 + m_x^2) \sin(\varphi - rm_y)] \right\}, \\ \dot{m}_z &= \frac{\omega_F}{1 + \alpha^2} \left\{ -Grm_x \sin(\varphi - rm_y) \right. \\ &\quad \left. - \alpha [Grm_y m_z \sin(\varphi - rm_y) - m_z (m_x^2 + m_y^2)] \right\}, \\ \frac{dV}{dt} &= \frac{1}{\beta_c} \left[I + A \sin(\omega_R t) - V - \sin(\varphi - rm_y) + r \frac{dm_y}{dt} \right], \\ \frac{d\varphi}{dt} &= V, \end{aligned} \quad (2)$$

where $\beta_c = 2eI_c CR^2/\hbar$ is the McCumber parameter (in our calculations we use $\beta_c = 25$); φ is the phase difference between the superconductors across the junction; $G = E_J/(KV)$; K is an anisotropic constant; \mathcal{V} is the volume of ferromagnetic F layer; $r = l v_{so}/v_F$ is parameter of SOC; v_{so}/v_F characterizes a relative strength of spin-orbit interaction; v_F is Fermi velocity; $l = 4hL/\hbar v_F$; L is the length of the F layer;

\hbar denotes the exchange field in the ferromagnetic layer; α is a phenomenological damping constant; $m_i = M_i/M_0$ for $i = x, y, z$; $M_0 = \|\mathbf{M}\|$; $\omega_F = \Omega_F/\omega_c$ with the FMR frequency $\Omega_F = \gamma K/M_0$; γ is the gyromagnetic ratio; characteristic frequency $\omega_c = 2eRI_c/\hbar$; A is the amplitude of external radiation normalized to I_c ; and ω_R is the frequency of external radiation normalized to ω_c . Here we normalize time in units of ω_c^{-1} , external current I in units of I_c , and voltage V in units of $V_c = I_c R$. The last term in the current equation shown in Eq. (2) was derived in the frame of microscopic theory for anomalous Josephson junction in Ref. [77]. In Ref. [78] the effect of this term was demonstrated.

This system of equations, solved numerically using the fourth-order Runge-Kutta method, yields $m_i(t)$, $V(t)$, and $\varphi(t)$ as a function of the external bias current I . After using the averaging procedure Refs. [79,80] we can find IVC at the fixed system's parameters.

III. RESULTS

A. FMR and effect of the SOC

Let us first discuss the effect of SOC on IVC and magnetization in our system. FMR in φ_0 JJ is demonstrated in Fig. 1(a), where we see an increase of magnetization amplitude m_y^{\max} (maximal m_y calculated at each value of the bias current) in the resonance region near $\omega_F = 0.5$. This resonance is also manifested in the IVC as the corresponding resonance branch shown by an arrow in this figure. We note that due to the nonlinearity in our system, which reflects the nonlinear nature of the LLG equation, the resonance frequency decreases with an increasing in SOC or damping in the system, i.e., the resonance realized at $\omega_J < \omega_F$ [81]. So, the end of the resonance branch does not coincide with ω_F . We see also that the manifestation of two FMR subharmonics corresponded to $V = \omega_F/2$ and $V = \omega_F/3$. The superconducting current which is demonstrated in this figure reflected the FMR also [61]. An increase in the SOC at small G and α , when the nonlinearity in LLG is getting stronger, leads also to the manifestation of nonlinearity in the IVC. It has a pronounced effect on the shape of the IV curve in the resonance region, represented as the deviation of the IV curve from its linear behavior and in the appearance of the resonance branch as shown in Fig. 1(b). A clear manifestation of a state with a NDR appears at $r > 0.4$.

An increase in the spin-orbit interaction increases also the peak in $m_y^{\max}(I)$ dependence and shifts it to the larger values of bias current as shown in Fig. 1(c). It is interesting to note that there are no clear indications of the transformation to the state with NDR in this dependence. But, as we see below, such manifestations appear under the external radiation.

B. Effect of the external radiation on the S/F/S φ_0 JJ

Due to Gilbert damping, the FMR frequency is decreased compared with the case at $\alpha = 0$; so to observe the effect of external radiation on IVC in the FMR region, we apply the radiation with a smaller frequency than $\omega_F = 0.5$ [81]. The results of calculations at $\omega_R = 0.485$ and amplitude $A = 0.1$ are presented in Fig. 2(a). It shows the voltage, the magnetization amplitude m_y^{\max} , and the superconducting current I_s

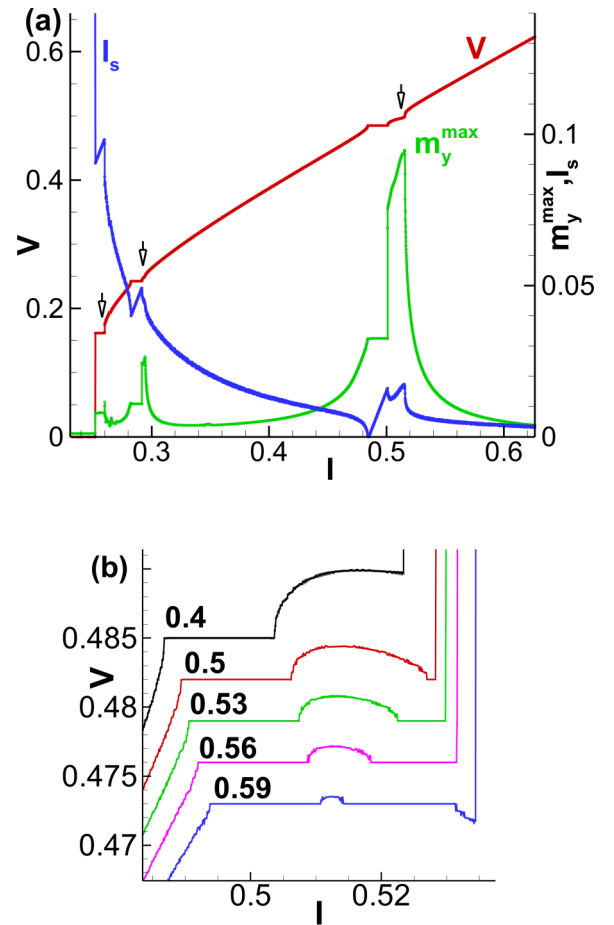


FIG. 2. (a) The same as in Fig. 1(a) under radiation with $\omega_R = 0.485$ and $A = 0.1$. (b) An enlarged view of the IV curves at different r . The curves are shifted down relatively the curve at $r = 0.4$ by $\Delta V = 0.003$.

plotted versus the bias current in its downward direction at a fixed value of SOC $r = 0.2$. We use the same parameters as in the case without radiation presented in Fig. 1(a). We see that the dependence $m_y^{\max}(I)$ demonstrates both phenomena, i.e., as the locking of magnetization precession and the FMR. The locking of Josephson oscillations to the radiation frequency is manifested as the SS in the IVC. The maximum of $m_y^{\max}(I)$ dependence demonstrates the FMR. The step in this dependence is actually a locking of magnetization precession to the oscillations of the external field through the locked Josephson oscillations. The average superconducting current obtained during the same numerical simulations demonstrates a specific feature of SS in Fig. 2(a). Thus $V(I)$, $m_y^{\max}(I)$, and $I_s(I)$ show clearly the features related to the FMR and locking of Josephson and magnetic oscillations to the oscillations of the external electromagnetic radiation.

The effect of external radiation on the IVC at different values of the SOC is demonstrated in Fig. 2(b) for fixed radiation frequency and amplitude. We see that the SS, a hump (dome) as a manifestation of the FMR, and the second SS appeared in the part of the resonance branch with NDR. We emphasize that the NDR state leads to a unique situation when two SS in the IVC coexist at the same frequency.

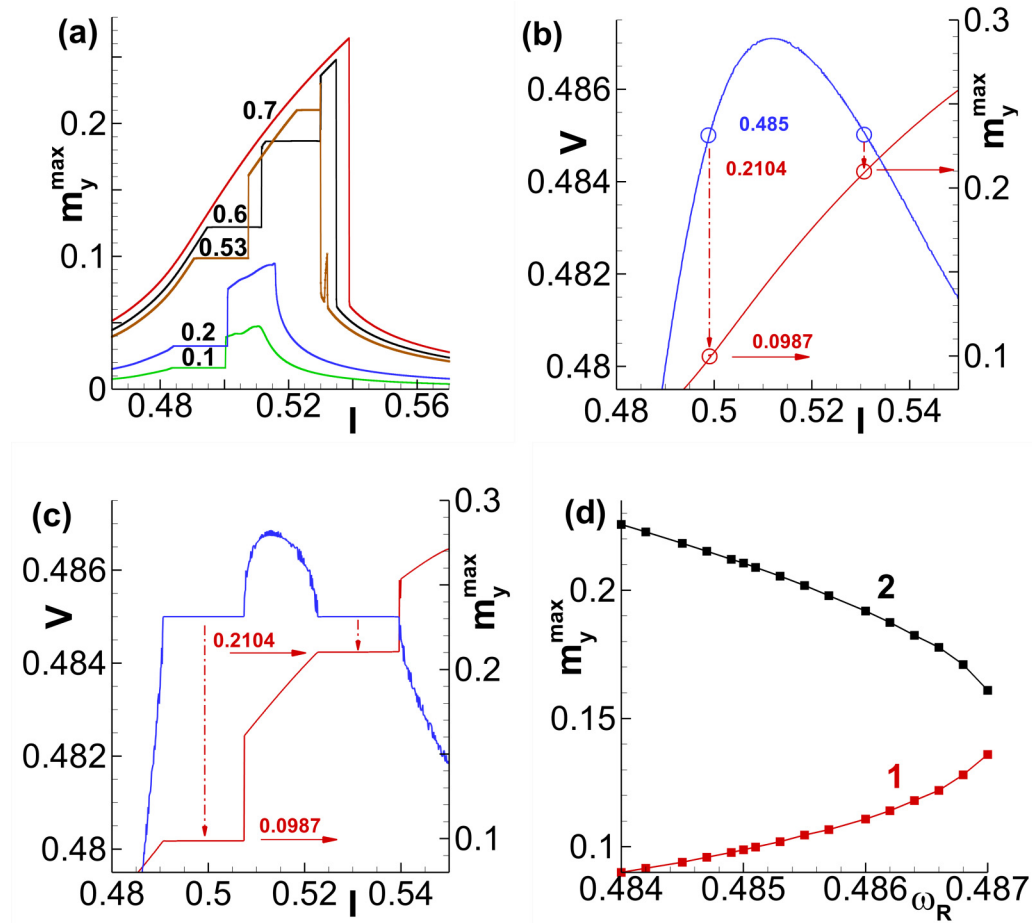


FIG. 3. (a) The bias current dependence of m_y^{\max} in the resonance region at different values of r under radiation with $\omega_R = 0.485$ and $A = 0.1$. (b) Procedure for locking steps determination (see text); (c) Results of numerical calculations of IVC and $m_y^{\max}(I)$ dependence under radiation with the same parameters. (d) Position of the locking steps in m_y^{\max} as a function of ω_R at $r = 0.53$ and $A = 0.12$. Lines are results of fitting by quadratic functions.

With an increase in the SOC, the maximum of the resonance curves presented in Fig. 1(b) is going down. Thus the appearance of the SS within the resonance branch can be observed for a certain range of the SOC parameter, in our case at $0 \leq r \leq 0.6$. For $r > 0.6$, the Josephson frequency ω_J is getting smaller than the radiation frequency $\omega_R = 0.485$ (due to the nonlinearity) and the maximum of the Josephson frequency is getting outside of the locking region, i.e., the Josephson oscillations go out from the locking conditions, which is why there are no SS at that r . We call this a “geometrical effect.”

C. Magnetization locking

The manifestation of the magnetic precession locking in the $m_y^{\max}(I)$ dependence and its variation with r are demonstrated in Fig. 3(a), where the curves with the specific features are shown. With an increase in the SOC in the interval $0.4 < r < 0.7$, the state with a NDR plays an essential role. It is reflected by an appearance of the second step in $m_y^{\max}(I)$ dependence that corresponds to the locking of magnetization precession at a higher value of m_y^{\max} . Thus two locking steps with the different maximal magnetization amplitude appear.

This situation is demonstrated in Fig. 3(a) by curves with $r = 0.53$ and $r = 0.6$.

A question appears regarding the position of the steps in $m_y^{\max}(I)$ dependence, i.e., the value of m_y^{\max} for the first and second steps. In contrast to the case of the Shapiro step, when its position depends only on the frequency of external radiation, the case of magnetization locking is more complicated. Of course, m_y^{\max} should also be determined by external radiation frequency. But in this case, it depends on the form resonance curve which depends on the parameters G , r , and α .

The procedure to find the position of the locking steps is demonstrated in Fig. 3(b). It shows the parts of the IV curve and $m_y^{\max}(I)$ dependence in the absence of external radiation. The value of radiation frequency $\omega_R = 0.485$ is marked by blue circles in the IV curve in the states with positive differential resistance and NDR. The bias current values in the IVC, which correspond to the voltage values ($V = \omega_r$), determine the position of the locking steps in $m_y^{\max}(I)$ dependence. The vertical lines, which pass through these points and cross the $m_y^{\max}(I)$ curve, fix the m_y^{\max} step positions at crossing points. In the discussed case, the first step is determined by value $m_y^{\max} = 0.0987$ and the second one (in the state with NDR) by $m_y^{\max} = 0.2104$. Figure 3(c) shows results of direct numerical calculations of IVC and $m_y^{\max}(I)$ dependence under radiation

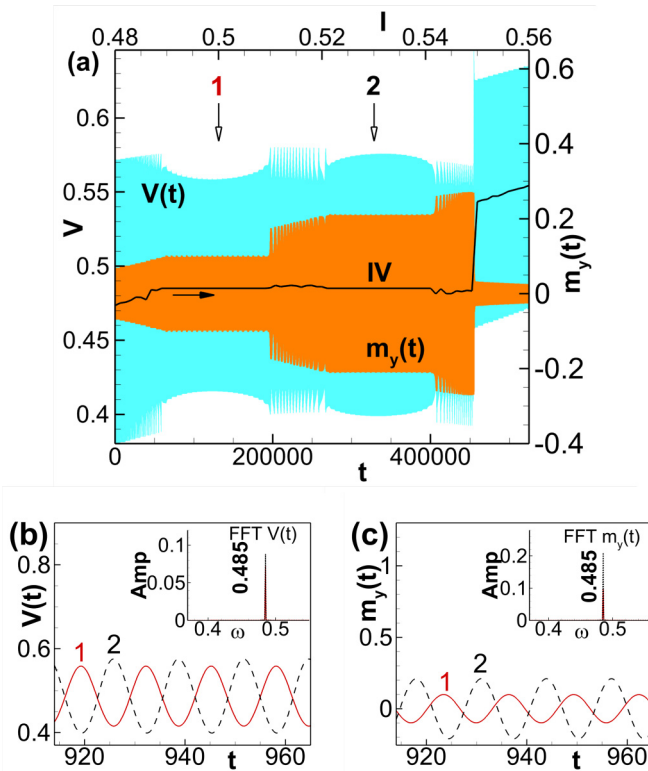


FIG. 4. (a) Enlarged resonance area of IVC together with the time dependence of voltage $V(t)$ and magnetization $m_y(t)$ at $G = 0.01$, $r = 0.53$, $\alpha = 0.01$, $A = 0.12$, and $\omega_R = 0.485$. The filled arrow denotes the direction of current change, the hollow arrows indicate the value of current at which the FFT has been performed. (b) Dynamics of voltage at current $I = 0.5$ (indicated as 1) and $I = 0.53$ (indicated as 2). The inset demonstrates the results of FFT analysis. (c) The same as (b) for m_y .

with $\omega_R = 0.485$ and $A = 0.1$ which demonstrates an agreement with the proposed procedure.

The width of the steps coincides with the width of the SS steps in both cases. From Fig. 3(b) it is clear that with an increase in ω_R the first step would go up, but the second one goes down because for the second step, when the blue circle goes up, the red one goes down. Results of the detailed step's position calculation as a function of radiation frequency and results of their fittings by quadratic function $a\omega_R^2 + b\omega_R + c$ with $a = 3623.1$, $b = -3504.2$, and $c = 847.37$ for the first step and $a = -3455.9$, $b = 3335.6$, and $c = -804.65$ for the second step are presented in Fig. 3(d).

D. Temporal dependence of $V(t)$ and m_y

An interesting effect can be seen in the time dependence of the voltage in the resonance branch region, which is shown in Fig. 4(a).

The amplitude $V(t)$ of the first SS decreases from the sides of the step to its middle while on the second SS it increases. This effect is caused by the state with NDR and appears because of the overlap of the FMR and locking conditions. Presented in Fig. 4(a), the time dependence of m_y in the resonance branch region confirms the locking of the magnetization

precession. The amplitude of oscillations of m_y rise on the resonance branch but in the SS region, the frequency and amplitude are fixed. Thus the magnetization at the second step oscillates with the ω_R but the amplitude of oscillations is larger than that at the first step.

The enlarged time dependence of voltage in both SS regions is demonstrated in Fig. 4(b). Due to the nonsynchronized nonlinear region between the steps, the oscillations are shifted in phase. As we mentioned already, the amplitude of oscillations is different because the second step is in the part of the resonance branch with NDR. The fast Fourier transform (FFT) analysis presented in the inset in Fig. 4(b) demonstrates the locking of m_y component in the both locking states is demonstrated in Fig. 4(c). The magnetic moment precesses with the same frequency but with different amplitudes. The FFT analysis of $m_y(t)$ time dependence in the locking region is presented in the inset in Fig. 4(c). It clearly shows one frequency ω_R which only confirms the locking of the magnetization precession by the external periodic drive.

IV. EFFECT OF NOISE ON THE LOCKING STEP

To simulate the experimental conditions, it is essential to check the effect of noise which might play an important role in different physical systems. Particularly, the random fluctuations are ubiquitous in the systems described by Josephson equations. In some cases the thermal noise has a crucial role in the dynamics of the Josephson phase. For example, in sensor applications it may alter the signal-to-noise resolution of the detector. It can act as a major source of decoherence for Josephson qubits [82] and the creation of vortex-antivortex pairs in the array of JJs [83]. The influence of thermal fluctuations as well as the role of Gaussian and nonGaussian noise sources on JJ systems are analyzed in Refs. [84–86]. In Refs. [38,87] the authors emphasize the thermal fluctuations of the current on the magnetization reversal phenomenon, where they have added the noise term in the current and effective field. An interesting effect of “softening” of the SS with an increase in noise amplitude was found in the rf-biased JJ [88].

In our case, to investigate the effect of noise on the appearance and stability of the locking steps, we have added a white noise to the bias current and effective field in the system of Eq. (2). We have tested the effect of noise with amplitude 10^{-5} which is normalized to the critical current I_c . We found that the locking phenomena discussed in this paper do not depend on the noise at chosen amplitude. Results are presented in Fig. 5. It shows the parts of IV characteristics and bias current dependence of m_y^{\max} in two cases: Without noise and with noise with amplitude 10^{-5} . As we see, the width of the locking steps and their positions do not change. Thus we expect that thermal noise would not make a strong effect on the locking steps in the φ_0 junction under external radiation in a real experiment.

V. CONCLUSION

To conclude, a method for controlling the dynamics of magnetization in the Josephson φ_0 junction is proposed. The

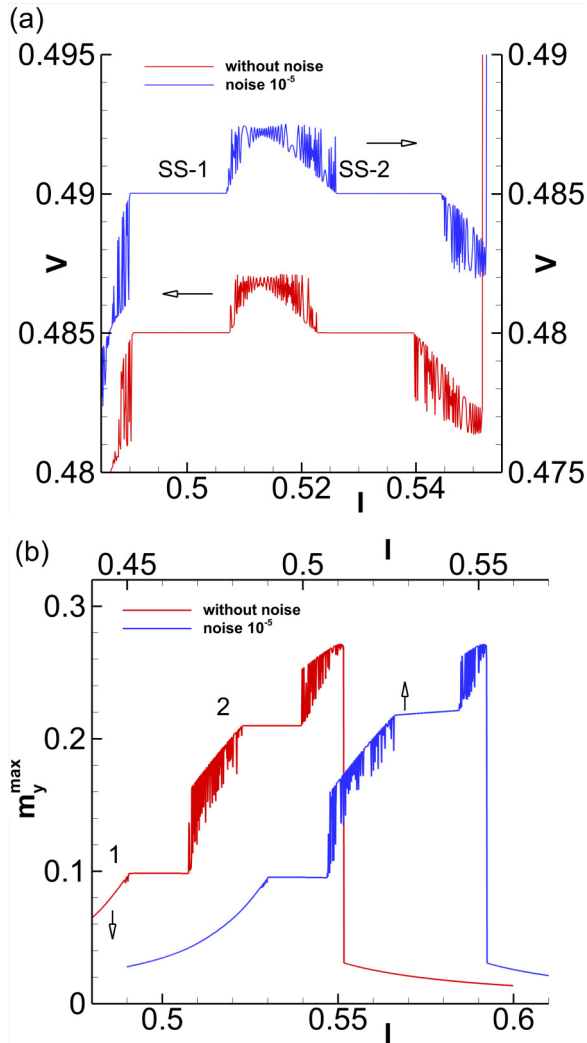


FIG. 5. (a) Demonstrates the enlarged SS in the IV-characteristic with noise 10^{-5} (blue line) and without noise (red line) at $G = 0.01$, $\alpha = 0.01$, $r = 0.53$, $\omega_R = 0.485$, $A = 0.1$. For clarity the blue curve is shifted up with value 0.05; (b) m_y^{\max} dependence at the same parameters as (a); for clarity, the blue curve is shifted to the right by value of 0.04.

possibility of locking the precession of magnetization by Josephson oscillations under external electromagnetic radiation is demonstrated. An additional locking step appears in a state with a NDR. The locking steps are determined by the frequency of external radiation and by the form of the FMR curve, which depends on the ratio of Josephson to magnetic energy, SOC, and Gilbert damping. The width of the locking steps is determined by amplitude of radiation and coincides with the width of SS in the IV characteristic. We have shown that external electromagnetic radiation can control not only the frequency of the magnetic precession but also its amplitude.

The experimental testing of our results would involve SFS structures with ferromagnetic material having enough strong SOC. Using superconductor-ferromagnetic insulator-superconductor on a 3D topological insulator might be a way to have the SOC needed for φ_0 JJ [89]. The interaction between the Josephson current and magnetization is determined by the ratio of the Josephson to the magnetic anisotropy energy $G = E_J/(KV)$ and spin-orbit interaction r . The value of the Rashba-type parameter r in a permalloy doped with Pt [90] and in the ferromagnets without inversion symmetry, like MnSi or FeGe, is usually estimated to be in the range 0.1 – 1. The value of the product Gr in the material with weak magnetic anisotropy $K \sim 4 \times 10^{-5} \text{ KA}^{-3}$ [91] and a junction with a relatively high critical current density of $(3 \times 10^5 - 5 \times 10^6) \text{ A/cm}^2$ [92] is in the range 1 – 100. It gives the set of ferromagnetic layer parameters that make it possible to reach the values used in our numerical calculations for the possible experimental observation of the predicted effects.

ACKNOWLEDGMENTS

The authors are grateful to I. R. Rahmonov for a fruitful discussion of the results of this paper. The study was carried out within the framework of the (ASRT, Egypt) (JINR, Russia) research projects. Numerical simulations were funded by Project No. 18-71-10095 of the Russian Science Foundation. Special thanks to BLTP, HybriLIT heterogeneous computing platform (LIT, JINR-Russia) and Bibliotheca Alexandrina (Egypt) for the HPC servers.

- [1] A. A. Golubov, M. Y. Kupriyanov, and E. Ilichev, The current-phase relation in Josephson junctions, *Rev. Mod. Phys.* **76**, 411 (2004).
- [2] A. I. Buzdin, Proximity effects in superconductor-ferromagnet heterostructures, *Rev. Mod. Phys.* **77**, 935 (2005).
- [3] F. S. Bergeret, A. F. Volkov, and K. B. Efetov, Odd triplet superconductivity and related phenomena in superconductor-ferromagnet structures, *Rev. Mod. Phys.* **77**, 1321 (2005).
- [4] S. Mai, E. Kandelaki, A. F. Volkov, and K. B. Efetov, Interaction of Josephson and magnetic oscillations in Josephson tunnel junctions with a ferromagnetic layer, *Phys. Rev. B* **84**, 144519 (2011).
- [5] J. Linder and J. Robinson, Superconducting spintronics, *Nat. Phys.* **11**, 307 (2015).
- [6] Yu. M. Shukrinov, Anomalous Josephson effect, *Phys.-Usp.* **65**, 317 (2022).
- [7] A. Zyuzin and B. Spivak, Theory of $\pi/2$ superconducting Josephson junctions, *Phys. Rev. B* **61**, 5902 (2000).
- [8] I. V. Krive, A. M. Kadigrobov, R. I. Shekhter, and M. Jonson, Influence of the Rashba effect on the Josephson current through a superconductor/Luttinger liquid/superconductor tunnel junction, *Phys. Rev. B* **71**, 214516 (2005).
- [9] V. Braude and Yu. V. Nazarov, Fully Developed Triplet Proximity Effect, *Phys. Rev. Lett.* **98**, 077003 (2007).
- [10] A. A. Reynoso, G. Usaj, C. A. Balseiro, D. Feinberg, and M. Avignon, Anomalous Josephson Current in Junctions with Spin Polarizing Quantum Point Contacts, *Phys. Rev. Lett.* **101**, 107001 (2008).

- [11] E. Goldobin, D. Koelle, R. Kleiner, and R. G. Mints, Josephson Junction with a Magnetic-Field Tunable Ground State, *Phys. Rev. Lett.* **107**, 227001 (2011).
- [12] M. Alidoust and J. Linder, Singlet-triplet superconducting quantum magnetometer, *Phys. Rev. B* **87**, 060503(R) (2013).
- [13] T. Yokoyama, M. Eto, and Y. V. Nazarov, Anomalous Josephson effect induced by spin-orbit interaction and Zeeman effect in semiconductor nanowires, *Phys. Rev. B* **89**, 195407 (2014).
- [14] E. Goldobin, D. Koelle, and R. Kleiner, Tunable $\pm\varphi$, φ_0 , and $\varphi_0\pm\varphi$ Josephson junction, *Phys. Rev. B* **91**, 214511 (2015).
- [15] A. Zyuzin, M. Alidoust, and D. Loss, Josephson junction through a disordered topological insulator with helical magnetization, *Phys. Rev. B* **93**, 214502 (2016).
- [16] M. Alidoust and H. Hamzehpour, Nonlocal Andreev entanglements and triplet correlations in graphene with spin-orbit coupling, *Phys. Rev. B* **96**, 165422 (2017).
- [17] M. Minutillo, D. Giuliano, P. Lucignano, A. Tagliacozzo, and G. Campagnano, Anomalous Josephson effect in S/SO/F/S heterostructures, *Phys. Rev. B* **98**, 144510 (2018).
- [18] M. Alidoust, M. Willatzen, and A.-P. Jauho, Fraunhofer response and supercurrent spin switching in black phosphorus with strain and disorder, *Phys. Rev. B* **98**, 085414 (2018).
- [19] M. Alidoust, Induced energy gap in finite-sized superconductor/ferromagnet hybrids, *Phys. Rev. B* **98**, 245418 (2018).
- [20] R. Mendiitto, M. Merker, M. Siegel, D. Koelle, R. Kleiner, and E. Goldobin, Evidence of macroscopic quantum tunneling from both wells in a φ Josephson junction, *Phys. Rev. B* **98**, 024509 (2018).
- [21] D. S. Shapiro, A. D. Mirlin, and A. Shnirman, Excess equilibrium noise in a topological SNS junction between chiral Majorana liquids, *Phys. Rev. B* **98**, 245405 (2018).
- [22] C. Spånslätt, Geometric Josephson effects in chiral topological nanowires, *Phys. Rev. B* **98**, 054508 (2018).
- [23] A. Buzdin, Direct Coupling Between Magnetism and Superconducting Current in the Josephson φ_0 Junction, *Phys. Rev. Lett.* **101**, 107005 (2008).
- [24] F. Konschelle and A. Buzdin, Magnetic Moment Manipulation by a Josephson Current, *Phys. Rev. Lett.* **102**, 017001 (2009).
- [25] J. Ferré, in *Spin Dynamics in Confined Magnetic Structures I*, edited by B. Hillebrands and K. Ounadjela (Springer-Verlag, Berlin, Heidelberg, 2002), Vol. 83, p. 127.
- [26] I. Žutić, J. Fabian, and S. Das Sarma, Spintronics: Fundamentals and applications, *Rev. Mod. Phys.* **76**, 323 (2004).
- [27] J. R. Hauptmann, J. Paaske, and P. E. Lindelof, Electric-field-controlled spin reversal in a quantum dot with ferromagnetic contacts, *Nat. Phys.* **4**, 373 (2008).
- [28] J.-F. Liu and K. S. Chan, Anomalous Josephson current through a ferromagnetic trilayer junction, *Phys. Rev. B* **82**, 125305 (2010).
- [29] J.-F. Liu, and K. S. Chan, Anomalous Josephson current through a ferromagnetic trilayer junction, *Phys. Rev. B* **82**, 184533 (2010).
- [30] Q. P. Herr, A. Y. Herr, O. T. Oberg, and A. G. Ioannidis, Ultra-low-power superconductor logic, *J. Appl. Phys.* **109**, 103903 (2011).
- [31] O. A. Mukhanov, Energy-efficient single flux quantum technology, *Trans. Appl.* **21**, 760 (2011).
- [32] B. Baek, W. H. Rippard, S. P. Benz, S. E. Russek, and P. D. Dresselhaus, Hybrid superconducting-magnetic memory device using competing order parameters, *Nat. Commun.* **5**, 3888 (2014).
- [33] N. O. Birge, A. E. Madden, and O. Naaman, Ferromagnetic Josephson junctions for cryogenic memory, *Spintronics XI* **124**, 10732 (2018).
- [34] F. Konschelle, I. V. Tokatly, and F. S. Bergeret, Semiclassical Quantization of Spinning Quasiparticles in Ballistic Josephson Junctions, *Phys. Rev. B* **92**, 125443 (2015).
- [35] Yu. M. Shukrinov, I. R. Rahmonov, K. Sengupta, and A. Buzdin, Magnetization reversal by superconducting current in φ_0 Josephson junctions, *Appl. Phys. Lett.* **110**, 182407 (2017).
- [36] M. Eschrig, Theory of Andreev bound states in S-F-S junctions and S-F proximity devices, *Philos. Trans. R. Soc. A* **376**, 20150149 (2018).
- [37] P. Kh. Atanasova, S. A. Panayotova, I. R. Rahmonov, Yu. M. Shukrinov, E. V. Zemlyanaya, and M. Bashashin, Periodicity in the appearance of intervals of the reversal of the magnetic moment of a φ_0 Josephson junction, *JETP Lett.* **110**, 722 (2019).
- [38] C. Guarcello and F. S. Bergeret, Cryogenic Memory Element Based on an Anomalous Josephson Junction, *Phys. Rev. Appl.* **13**, 034012 (2020).
- [39] M.-H. Nguyen, G. J. Ribeill, M. Gustafsson, Sh. Shi, S. V. Aradhya, A. P. Wagner, L. Ranzani, L. Zhu, R. Baghdadi, B. Butters, E. Toomey, M. Colangelo, P. A. Truitt, A. Jafari-Salim, D. McAllister, D. Yohannes, S. R. Cheng, R. Lazarus, O. A. Mukhanov, K. K. Berggren, R. A. Buhrman, G. E. Rowlands, and T. A. Ohki, Cryogenic memory architecture integrating spin hall effect based magnetic memory and superconductive cryotron devices, *Sci. Rep.* **10**, 248 (2020).
- [40] A. A. Mazanik, I. R. Rahmonov, A. E. Botha, and Yu. M. Shukrinov, Analytical Criteria for Magnetization Reversal in a φ_0 Josephson junction, *Phys. Rev. Appl.* **14**, 014003 (2020).
- [41] D. B. Szombati, S. Nadj-Perge, D. Car, S. R. Plissard, E. P. A. M. Bakkers, and L. P. Kouwenhoven, Josephson φ_0 junction in nanowire quantum dots, *Nat. Phys.* **12**, 568 (2016).
- [42] A. Assouline, C. Feuillet-Palma, N. Bergeal, T. Zhang, A. Mottaghizadeh, A. Zimmers, E. Lhuillier, M. Eddrie, P. Atkinson, M. Aprili, and H. Aubin, Spin-Orbit induced phase-shift in Bi₂Se₃ Josephson junctions, *Nat. Commun.* **10**, 126 (2019).
- [43] W. Mayer, M. C. Dartiaill, J. Yuan, K. S. Wickramasinghe, E. Rossi, and J. Shabani, Gate controlled anomalous phase shift in Al/InAs Josephson junctions, *Nat. Commun.* **11**, 212 (2020).
- [44] J. Alicea, New directions in the pursuit of Majorana fermions in solid state systems, *Rep. Prog. Phys.* **75**, 076501 (2012).
- [45] A. Fornieri, A. M. Whiticar, F. Setiawan, E. Portolés, A. C. C. Drachmann, A. Keselman, S. Gronin, C. Thomas, T. Wang, R. Kallagher, G. C. Gardner, E. Berg, M. J. Manfra, A. Stern, C. M. Marcus, and F. Nichele, Evidence of topological superconductivity in planar Josephson junctions, *Nature* **569**, 89 (2019).
- [46] H. Ren, F. Pientka, S. Hart, A. T. Pierce, M. Kosowsky, L. Lunczer, R. Schlereth, B. Scharf, E. M. Hankiewicz, L. W. Molenkamp, B. I. Halperin, and A. Yacoby, Topological superconductivity in a phase-controlled Josephson junction, *Nature* **569**, 93 (2019).
- [47] L. Cai and E. M. Chudnovsky, Interaction of a nanomagnet with a weak superconducting link, *Phys. Rev. B* **82**, 104429 (2010).
- [48] E. M. Chudnovsky, Quantum decay of the persistent current in a Josephson junction ring, *Phys. Rev. B* **93**, 144422 (2016).

- [49] X. Waintal and P. W. Brouwer, Magnetic exchange interaction induced by a Josephson current, *Phys. Rev. B* **65**, 054407 (2002).
- [50] V. Braude and Ya. M. Blanter, Triplet Josephson Effect with Magnetic Feedback in a Superconductor-Ferromagnet Heterostructure, *Phys. Rev. Lett.* **100**, 207001 (2008).
- [51] J. Linder and T. Yokoyama, Anomalous magnetic transport in ferromagnetic graphene junctions, *Phys. Rev. B* **83**, 012501 (2011).
- [52] C. Holmqvist, M. Fogelström, and W. Belzig, Spin-polarized Shapiro steps and spin-precession-assisted multiple Andreev reflection, *Phys. Rev. B* **90**, 014516 (2014).
- [53] B. Abdollahipour, Abouie, and N. Ebrahimi, Shapiro like steps reveals molecular nanomagnets' spin dynamics, *AIP Adv.* **5**, 097156 (2015).
- [54] C. Holmqvist, W. Belzig, and M. Fogelström, Non-equilibrium charge and spin transport in superconducting-ferromagnetic-superconducting point contacts, *Philos. Trans. R. Soc. A* **376**, 20150229 (2018).
- [55] F. S. Bergeret, M. Silaev, P. Virtanen, and T. T. Heikkilä, Colloquium: Nonequilibrium effects in superconductors with a spin-splitting field, *Rev. Mod. Phys.* **90**, 041001 (2018).
- [56] B. Lu, P. Bursert, and Y. Tanaka, Spin-polarized multiple Andreev reflections in spin-split superconductors, *Phys. Rev. B* **101**, 020502(R) (2020).
- [57] R. Ojajärvi, J. Manninen, T. T. Heikkilä, and P. Virtanen, Nonlinear spin torque, pumping, and cooling in superconductor/ferromagnet systems, *Phys. Rev. B* **101**, 115406 (2020).
- [58] S. V. Mironov and A. I. Buzdin, Collective magnetic and plasma excitations in Josephson ψ junctions, *Phys. Rev. B* **104**, 134502 (2021).
- [59] A. Villas, R. L. Klees, G. Morrás, H. Huang, C. R. Ast, G. Rastelli, W. Belzig, and J. C. Cuevas, Tunneling processes between Yu-Shiba-Rusinov bound states, *Phys. Rev. B* **103**, 155407 (2021).
- [60] H. Hammar and J. Fransson, Time-dependent spin and transport properties of a single-molecule magnet in a tunnel junction, *Phys. Rev. B* **94**, 054311 (2016).
- [61] Yu. M. Shukrinov, I. R. Rahmonov, and K. Sengupta, Ferromagnetic resonance and magnetic precessions in $\phi 0$ junctions, *Phys. Rev. B* **99**, 224513 (2019).
- [62] J. Nagel, D. Speer, T. Gaber, A. Sterck, R. Eichhorn, P. Reimann, K. Ilin, M. Siegel, D. Koelle, and R. Kleiner, Observation of Negative Absolute Resistance in a Josephson Junction, *Phys. Rev. Lett.* **100**, 217001 (2008).
- [63] N. F. Pedersen, G. Filatrella, V. Pierro, and M. P. Sørensen, Negative differential resistance in Josephson junctions coupled to a cavity, *Physica C* **503**, 178 (2014).
- [64] K. Kadowaki, H. Yamaguchia, K. Kawamata, T. Yamamoto, H. Minami, I. Kakeya, U. Welp, L. Ozyuzer, A. Koshelev, C. Kurter, K. E. Gray, and W.-K. Kwok, Direct observation of tetrahertz electromagnetic waves emitted from intrinsic Josephson junctions in single crystalline $\text{Bi}_2\text{Sr}_2\text{CaCu}_2\text{O}_{8+\delta}$, *Physica C* **468**, 634 (2008).
- [65] S.-Z. Lin and A. E. Koshelev, Linewidth of the electromagnetic radiation from Josephson junctions near cavity resonances, *Phys. Rev. B* **87**, 214511 (2013).
- [66] Y.-C. Lin, R. K. Ghosh, R. Addou, N. Lu, S. M. Eichfeld, H. Zhu, M.-Y. Li, X. Peng, M. J. Kim, L.-J. Li, R. M. Wallace, S. J. Datta, and A. Robinson, Atomically thin resonant tunnel diodes built from synthetic van der Waals heterostructures, *Nat. Commun.* **6**, 7311 (2015).
- [67] W. S. Choi, S. A. Lee, J. H. You, S. Lee, and H. N. Lee, Resonant tunnelling in a quantum oxide superlattice, *Nat. Commun.* **6**, 7424 (2015).
- [68] P. M. Campbell, A. Tarasov, C. A. Joiner, W. J. Ready, and E. M. Vogel, Enhanced Resonant Tunneling in Symmetric 2D Semiconductor Vertical Heterostructure Transistors, *ACS Nano* **9**, 5000 (2015).
- [69] T. Roy, M. Tosun, X. Cao, H. Fang, D.-H. Lien, P. Zhao, Y.-Z. Chen, Y.-L. Chueh, J. Guo, and A. Javey, Dual-Gated $\text{MoS}_2/\text{WSe}_2$ van der Waals tunnel diodes and transistors, *ACS Nano* **9**, 2071 (2015).
- [70] J. Shim, S. Oh, D.-H. Kang, S.-H. Jo, M. H. Ali, W.-Y. Choi, K. Heo, J. Jeon, S. Lee, M. Kim, Y. J. Song, and J.-H. Park, Phosphorene/rhenium disulfide heterojunction-based negative differential resistance device for multi-valued logic, *Nat. Commun.* **7**, 13413 (2016).
- [71] P. M. Campbell, A. Tarasov, C. J. Joiner, W. J. Ready, and E. M. Vogel, Band structure effects on resonant tunneling in III-V quantum wells versus two-dimensional vertical heterostructures, *J. Appl. Phys.* **119**, 024503 (2016).
- [72] K. Kobashi, R. Hayakawa, T. Chikyow, and Y. Wakayama, Multi-Valued logic circuits based on organic anti-ambipolar transistors, *Nano Lett.* **18**, 4355 (2018).
- [73] K. H. Kim, H. Y. Park, J. Shim, G. Shin, M. Andreev, J. Koo, G. Yoo, K. Jung, K. Heo, Y. Lee, and H. Y. Yu, A multiple negative differential resistance heterojunction device and its circuit application to ternary static random access memory, *Nanoscale Horiz.* **5**, 654 (2020).
- [74] M. Smidman, M. B. Salamon, H. Q. Yuan, and D. F. Agterberg, Superconductivity and spin-orbit coupling in non-centrosymmetric materials: A review, *Rep. Prog. Phys.* **80**, 036501 (2017).
- [75] Y. Yanase and M. Sigrist, Superconductivity and Magnetism in Non-centrosymmetric System: Application to CePt_3Si , *J. Phys. Soc. Jpn.* **77**, 124711 (2008).
- [76] Y. Yanase, Electronic structure and noncentrosymmetric superconductivity in three-orbital t_{2g} model with spin-orbit coupling: Sr_2RuO_4 near [001] surface/interface, *J. Phys. Soc. Jpn.* **82**, 044711 (2013).
- [77] D. S. Rabinovich, I. V. Bobkova, A. M. Bobkov, and M. A. Silaev, Resistive State of Superconductor-Ferromagnet-Superconductor Josephson Junctions in the Presence of Moving Domain Walls, *Phys. Rev. Lett.* **123**, 207001 (2019).
- [78] Yu. M. Shukrinov and I. R. Rahmonov, Resonance properties of the Josephson junctions with ferromagnets, *Phys. Part. Nucl.* **51**, 816 (2020).
- [79] Yu. M. Shukrinov, F. Mahfouzi, and N. F. Pedersen, Investigation of the breakpoint region in stacks with a finite number of intrinsic Josephson junctions, *Phys. Rev. B* **75**, 104508 (2007).
- [80] W. Buckel and R. Kleiner, *Superconductivity: Fundamentals and Applications* (John Wiley & Sons, 2008).
- [81] Yu. M. Shukrinov, I. R. Rahmonov, A. Janalizadeh, and M. R. Kollahchi, Anomalous Gilbert damping and Duffing features of the superconductor-ferromagnet-superconductor $\phi 0$ Josephson junction, *Phys. Rev. B* **104**, 224511 (2021).
- [82] J. Lisenfeld, A. Lukashenko, M. Ansmann, J. M. Martinis, and A. V. Ustinov, Temperature Dependence of Coherent

- Oscillations in Josephson Phase Qubits, *Phys. Rev. Lett.* **99**, 170504 (2007).
- [83] T. P. Orlando, J. E. Mooij, and H. S. J. van der Zant, Phenomenological model of vortex dynamics in arrays of Josephson junctions, *Phys. Rev. B* **43**, 10218 (1991); D. J. Resnick, J. C. Garland, J. T. Boyd, S. Shoemaker, and R. S. Newrock, Kosterlitz-Thouless Transition in Proximity-Coupled Superconducting Arrays, *Phys. Rev. Lett.* **47**, 1542 (1981).
- [84] C. Guarcello, D. Valenti, and B. Spagnolo, Phase dynamics in graphene-based Josephson junctions in the presence of thermal and correlated fluctuations, *Phys. Rev. B* **92**, 174519 (2015).
- [85] C. Guarcello, D. Valenti, A. Carollo, and B. Spagnolo, Stabilization effects of dichotomous noise on the lifetime of the superconducting state in a long Josephson junction, *Entropy* **17**, 2862 (2015).
- [86] C. Guarcello, D. Valenti, B. Spagnolo, V. Pierro, and G. Filatrella, Anomalous transport effects on switching currents of graphene-based Josephson junctions, *Nanotechnology* **28**, 134001 (2017).
- [87] C. Guarcello and F. S. Bergeret, Thermal noise effects on the magnetization switching of a ferromagnetic anomalous Josephson junction, *Chaos, Solitons Fractals* **142**, 110384 (2021).
- [88] A. K. Chattah, C. B. Briozzo, O. Osenda, and M. O. Cáceres, Effect of thermal noise on the current-voltage characteristics of Josephson junctions, *Mod. Phys. Lett. B* **10**, 1095 (1996).
- [89] I. V. Bobkova, A. M. Bobkov, I. R. Rahmonov, A. A. Mazanik, K. Sengupta, and Yu. M. Shukrinov, Magnetization reversal in superconductor/insulating ferromagnet/superconductor Josephson junctions on a three-dimensional topological insulator, *Phys. Rev. B* **102**, 134505 (2020).
- [90] A. Hrabec, F. J. T. Goncalves, C. S. Spencer, E. Arenholz, A. T. N'Diaye, R. L. Stamps, and C. H. Marrows, Spin-orbit interaction enhancement in permalloy thin films by Pt doping, *Phys. Rev. B* **93**, 014432 (2016).
- [91] A. Yu. Rusanov, M. Hesselberth, J. Aarts, and A. I. Buzdin, Enhancement of the Superconducting Transition Temperature in Nb/Permalloy Bilayers by Controlling the Domain State of the Ferromagnet, *Phys. Rev. Lett.* **93**, 057002 (2004).
- [92] J. W. A. Robinson, F. Chiodi, M. Egilmez, G. B. Halász, and M. G. Blamire, Supercurrent enhancement in Bloch domain walls, *Sci. Rep.* **2**, 699 (2012).